Structures and energetics for polar and nonpolar SiC surface relaxations

S. P. Mehandru and Alfred B. Anderson*
Chemistry Department, Case Western Reserve University, Cleveland, Ohio 44106
(Received 10 January 1990; revised manuscript received 28 June 1990)

We have investigated the nature of relaxations and resultant stability gains for polar (both Si- and C-terminated) and nonpolar (equal concentration of Si and C) surfaces of zinc-blende (cubic) and wurtzite (hexagonal) surfaces of SiC, using the tight-binding atom-superposition and electron-delocalization band technique. The ideally truncated C surfaces of (111) and (100) β-SiC are predicted to exhibit larger inward displacements and stabilizations than the Si surfaces, which is in agreement with the semiempirical total-energy band calculations of Lee and Joannopoulos but not with the empirical potential-function prediction of Takai *et al.* The inward displacements on these surfaces have associated with them increased surface-atom–to–substrate σ-bonding stabilization and the destabilization of the dangling surface-state band on the (111) surfaces and of both dangling surface-state bands on the (100) surfaces. The Si- and C-terminated (100) surfaces are calculated to undergo dimerizations similar to those observed on the Si(100) and C(100) surfaces with σ-bond formation and some stabilizing π overlap of the remaining surface dangling orbitals. The atoms on the nonpolar surfaces each have a single dangling surface orbital, empty for Si and doubly occupied for C. The relaxations at the β-SiC(110) surface show a combination of buckling and downward displacement. The zig-zag chains in the surface plane acquire some π character due to bonding overlaps between the dangling sp-hybrid surface orbitals on surface Si and C atoms along the chains. The relaxed α-SiC($10\bar{1}0$) surface displays buckled and asymmetric SiC dimers on the surface with contracted bond distance, again due to in-phase π overlaps between the sp-hybridized dangling surface orbitals on dimer atoms. The relaxation pattern and ensuing stability for the α-SiC($11\bar{2}0$) surface are intermediate between those for the β-SiC(110) and α-SiC($10\bar{1}0$) surfaces and is explained on the basis of the geometric structure and the directions of the dangling surface-state orbitals on neighboring surface atoms, which lead to intermediate π stabilization.

I. INTRODUCTION

The (100) surfaces of technologically important tetrahedrally coordinated group-IV materials such as Si and Ge have been a focus of attention during the past decade, both experimentally[1–10] and theoretically.[11–19] It is now known that the clean unrelaxed (100) surfaces of Si and Ge undergo restructuring with dimerization in the top surface layer, which causes the observed (2×1) low-energy electron diffraction (LEED) pattern. The driving force for dimer formation is the stability gain accompanying bond formation between neighboring surface atoms while maintaining the bonds with atoms in the layer underneath. This is accompanied by a reduction in the surface dangling orbitals from two per surface atom for the bulk-terminated (100) surfaces to one per atom following dimerization. Knowledge of the detailed configuration of dimers (symmetric versus asymmetric) has a degree of uncertainty. While the early total-energy calculations[11–19] and LEED experiments[1] indicated an asymmetric and buckled dimer structure, the more recent scanning tunneling microscope (STM) investigation showed symmetric dimers on defect-free Si(100).[5] Very recent total-energy and core-level-shift calculations[20] using the unrestricted Hartree-Fock approximation have predicted symmetric dimers on the Si(100)-(2×1) surface, as did slab calculations[21] using the modified intermediate neglect of differential overlap (MINDO) method and self-consistent-field (SCF) pseudopotential calculations.[22]

The clean (111) surfaces of Si, Ge, and diamond also exhibit (2×1) reconstruction.[23–33] Several models have been proposed for this restructuring, including the Haneman buckled model,[30] the Seiwatz single-chain model,[31] the Chadi π-bonded molecule model,[32] and the Pandey π-chain model.[29] The currently favored Pandey π-chain model involves comparatively large changes in the bonding topology of the top two layers in a manner which brings the dangling orbitals on the nearest-neighbor atoms close to one another, resulting in π-bond formation (sp^2-hybridized surface atoms) along the chain. It may be mentioned that the relaxations of the other index planes of Si, Ge, and C have not attracted much attention.

SiC is tetrahedrally bonded high-strength structural material which also has potential applications in high-temperature electronic devices. Knowledge of its surface structures is not only of technological importance but also of scientific interest because two group-IV elements of different electronegativities participate in bonding. Due to the expected charge transfer from Si to C, various polar and nonpolar surfaces containing Si cations and C anions, can, in principle, be formed. In practice it is difficult to prepare the idealized homogeneous, ordered, and stoichiometric SiC surfaces, and because of the variability in surface properties that can be achieved by chemical preparation, such surfaces are referred to as phases. Based on Auger and LEED measurements, Dayan[34] con-

cluded that his C-terminated phase of β-SiC(100) was (2×1) reconstructed, similar to the (100) surfaces of Si and Ge. The Si-rich phase prepared by Kaplan exhibited $c(2\times2)$, (2×1), (3×2), and $c(4\times2)$ LEED patterns.[35] Only the $c(4\times2)$ and (2×1) phases were found to have a complete Si-atom layer, and a buckled Si-dimer structure similar to that on Si(100) was proposed for this surface.[35] Surface structures of the other phases are not known so far. A similar lack of knowledge about surface structures exists for the basal plane β-SiC(111) and α-SiC(0001) surfaces. As expected on the basis of structural similarity, these surfaces exhibited identical (3×3), $(\sqrt{3}\times\sqrt{3})R\,30°$, and (1×1) LEED patterns,[35] but the surface structures for these phases are not known. Lee and Joannopoulos[36] have calculated relaxation energies and structures for idealized nonpolar β-SiC(110), α-SiC$(10\bar{1}0)$, and $(11\bar{2}0)$ surfaces using a semiempirical total-energy-band technique. Takai *et al.*[37] have used empirically parametrized analytical potential-energy functions to calculate relaxation energies for the polar (100) and (111) and nonpolar (110) β-SiC surfaces. While relaxations were evidently calculated in Ref. 37, the only reported results are that on the β-SiC(110) surface the C atoms relax down farther than the Si atoms, which is opposite to the result obtained in Ref. 36.

In this paper we report the results of a relatively extensive theoretical multilayer surface relaxation investigation of the polar (111) and (100) and nonpolar β-SiC(110) surfaces, and for the nonpolar $(10\bar{1}0)$ and $(11\bar{2}0)$ surfaces of α-SiC. The tight-binding atom-superposition and electron-delocalization (ASED)-band method is employed.

II. METHOD

The ASED-band technique is a generalization of the ASED molecular-orbital (MO) theory[38] which has been applied in recent years to different types of surface problems by using finite-sized cluster models. The ASED-MO method is semiempirical and based on partitioning the molecular electronic charge-density distribution function $\rho_{\rm mol}$ into rigid atomic components ρ_i's and a nonrigid bond charge delocalization component ρ_D. Thus for a diatomic molecule *a*-*b* (generalization to polyatomics and solids is straightforward)

$$\rho_{\rm mol}=\rho_a+\rho_b+\rho_D \ .$$

From the electrostatic theorem, there are two nonzero components to the force on nucleus a in the molecule: an attractive force due to ρ_D, and a repulsive force due to atom b (ρ_b and the nuclear charge Z_b). Integrating these forces as the atoms come together forming bonds yields an attractive energy E_D due to electron delocalization, and repulsive energy E_R due to atom superposition. The total energy as a function of internuclear distance r is given by

$$E(r)=E_R(r)+E_D(r) \ .$$

The two-body repulsion energy E_R is readily obtained from available Slater-type atomic functions.[39] E_D is approximated as the difference between the valence-electron orbital energies for the atoms[40] and the molecular orbital energies of the valence electrons as determined from an extended Hückel-like molecular Hamiltonian which is dependent on the Slater orbitals and ionization potentials. The Slater-orbital exponents and ionization potentials may be changed so that the calculations produce proper diatomic bond lengths and bond ionicities. The ASED-MO method is thus a simply way to predict molecular structures, bond strengths, force constants, electronic structures, and orbitals. The ASED-band method[41] is a bulk band version of the ASED-MO method and can be used to model extended two- and three-dimensional systems for studying surface and bulk properties, respectively.

In a recent study of cubic and hexagonal SiC,[41] Si and C Slater exponents obtained from the SCF calculations of Clementi and Raimondi[39] were scaled to produce the experimental bulk Si-C distance (within 0.01 Å) using the tight-binding approach in the ASED framework. At the same time, the experimental valence-state ionization potentials of Si and C were, respectively, increased and decreased by 1.3 eV to produce the expected charge transfer from Si to C based on their electronegativity difference. The same atomic parameters were recently employed to study the bonding and adhesion of SiC and AlN surfaces using infinite slabs,[42] as well as in the interfacial binding study of polar and nonpolar SiC surfaces with close-packed Ti(0001) using large cluster models.[43] We use the same parameters in the present investigation. These parameters have been shown[41] to produce reasonable bulk properties for cubic (3*C*) β-SiC and hexagonal (2*H*) α-SiC when used in the ASED-band framework. For β-SiC the calculated atomization energy, bulk modulus, and band gap are 12.0 eV, 261 GPa, and 3.71 eV, respectively, compared to the respective experimental values of 12.71 eV, 224 GPa, and 2.39 eV. For α-SiC the same atomic parameters yielded values of 11.96 eV, 264 GPa, and 3.55 eV for these properties as compared to 12.69 eV, 225 GPa, and 3.3 eV, respectively, from experiment.

While studying relaxations on one face of a slab, the other face was saturated with H atoms. The experimental Si-H and C-H bond distances of 1.48 and 1.09 Å, respectively, were employed. The overlap integrals used in constructing the Bloch Hamiltonian are calculated for atoms with centers up to 10 Å apart. 100 k points in the full Brillouin zone were found to be sufficient for energy convergence. Simpson's rule was used to determine the band energy by integration over the electronic density of states.

III. RELAXATIONS ON POLAR SiC SURFACES

In this section the results for the Si-terminated and the C-terminated polar (111) and (100) β-SiC surface relaxations are presented. For the (111) surfaces each surface Si(C) is coordinated to three C(Si) in the layer underneath, as shown in Fig. 1. As suggested by Lee and Joannopoulos,[36] it will be energetically favorable for an atom with s^2p^2 valence electronic configuration having three bonds to have a planar structure (sp^2 hybridization) and

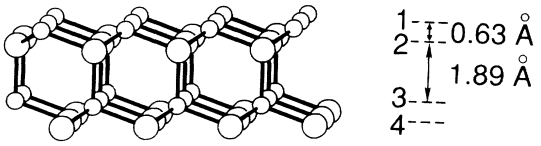

FIG. 1. Side view of a piece of the β-SiC(111) surface double layer and the first bulk double layer beneath it. Atom layer 1 is at the surface and layers 2, 3, and 4 lie beneath. The smaller spheres represent Si atoms.

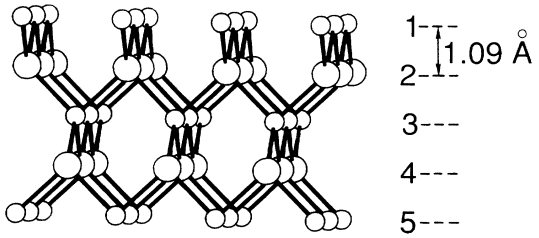

FIG. 2. Five-layer slab of β-SiC with layer 1 representing a (100) surface.

one electron in the p orbital perpendicular to the plane. The (111) surface Si (or C) atoms are, therefore, expected to undergo downward displacement toward a planar configuration with the next layer atoms. Since the second-layer atoms are constrained by the bulk lattice, the surface atoms will not be able to assume an exactly planar geometry. Nevertheless, there will be an optimal vertical relaxation of the top layer and the influence of the surface is expected to extend more than one layer into the bulk, with rapidly decreasing vertical displacements. For the β-SiC(100) Si and C surfaces, each surface Si(C) has two bonds to atoms of the opposite kind in the second layer (see Fig. 2). Applying the above arguments based on atomic valence-electron configuration to these surface atoms, one expects a driving force toward forming sp-hybridized linear bonds involving the next layer atoms and two singly occupied orthogonal p orbitals. The surface atoms, therefore, ought to show downward relaxation, and there should be smaller relaxations extending to some distance into the bulk. It may be noted that a linear combination of the nonbonded orthogonal p orbitals on the (100) surface atoms will give rise to two singly occupied surface dangling orbitals along the cleaved bond directions. Furthermore, the polar β-SiC(100) surfaces are expected to exhibit lateral displacement of surface-layer atoms resulting in dimer formation, as has been observed on the clean (100) surfaces of Si and Ge. We have investigated vertical relaxations on the (111) and (100) β-SiC surfaces as well as symmetrical dimer formation on the Si and the C-terminated β-SiC(100) surfaces. These results are presented in this section.

A. Vertical relaxations on (111) and (100) β-SiC

For studying vertical relaxations, ten-layer-thick slabs were employed. The unit cells for the Si-terminated and the C-terminated basal plane (111) surfaces consisted of 5 Si, 5 C, and 2 H atoms, and for the (100) surface they had one additional H atom. For each surface the top five layers were relaxed up and down to the nearest 0.01 Å, while the remaining five layers were kept fixed at the bulk positions.

As discussed previously,[42] the (111) surface-state bands are narrow, $\sim$0.4 eV for C and $\sim$1.0 eV for Si, so it is assumed that each surface-band orbital is occupied by one electron as was done before. For the (100) surfaces the calculated surface bands are wider, $\sim$3.0 eV for C and 4.5 eV for Si, before relaxation, so there is a chance that there will be no half-filled surface orbitals, but just doubly filled ones. Because of this, two sets of results are given in the tables for the (100) surfaces, but the low-spin doubly occupied surface orbital results are more likely to correspond to the actual surfaces, and these results are the basis of discussion in the text.

Calculated results for multilayer relaxations are given in Table I. It may be seen that the magnitudes of vertical surface relaxations and the resultant stabilizations per

TABLE I. Relaxation energies per surface atom and structures calculated for the vertical relaxations of polar β-SiC (111) and (100) surfaces. ΔE is the stability gain per surface atom, Δh_n is the nth-layer displacement from the bulk lattice position, and Δd_{nm} is the percent change in interlayer spacing between the nth and mth layers from the bulk value. Negative (positive) signs represent downward (upward) displacement from bulk positions. Spin paired results for the (100) surface are in parentheses.

	β-SiC(111)		β-SiC(100)	
	Si surface	C surface	Si surface	C surface
ΔE (eV)	0.03	0.43	0.02(0.03)	0.34(0.21)
Δh_1 (Å)	−0.05	−0.21	−0.04(−0.05)	−0.17(−0.15)
Δd_{12} (%)	−11.1	−52.4	−4.6(−5.5)	−22.0(−17.4)
Δh_2 (Å)	0.02	0.12	0.01(0.01)	0.07(0.04)
Δd_{23} (%)	9.5	36.5	4.6(4.6)	12.8(10.1)
Δh_3 (Å)	−0.04	−0.11	−0.04(−0.04)	−0.07(−0.07)
Δd_{34} (%)	−6.4	−19.1	−3.7(−3.7)	−6.4(−6.4)
Δh_4 (Å)	0.0	0.01	0.0(0.0)	0.0(0.0)
Δd_{45} (%)	1.6	6.4	0.0(0.0)	1.8(1.8)
Δh_5 (Å)	−0.01	−0.03	0.0(0.0)	−0.02(−0.02)

TABLE II. Relaxation energies and structures calculated for the β-SiC(100) surfaces, assuming both spin pairing in the surface orbitals and spin unpairing. Empirical potential function prediction of the dimerization atom energies of Takai *et al.* (Ref. 37) are also given. ΔX_1 and ΔX_2 are first- and second-layer lateral relaxation distances along the [110] direction; other parameters are defined in Table I.

	Si surface		C surface	
	Spin paired	Spin unpaired	Spin paired	Spin unpaired
Stability/ dimer (eV)	1.03	3.80	1.22	2.31
	0.74 (Takai)		3.46 (Takai)	
R (dimer) (Å)	2.16	2.21	1.74	1.74
ΔX_1 (Å)	0.46	0.44	0.67	0.67
ΔX_2 (Å)	0.02	0.05	0.07	0.07
Δh_1 (Å)	−0.10	−0.05	−0.19	−0.19
Δd_{12} (%)	−11.9	−6.4	−21.1	−22.0
Δh_2 (Å)	0.03	0.02	0.04	0.05
Δd_{23} (%)	4.6	2.8	7.3	8.3
Δh_3 (Å)	−0.02	−0.01	−0.04	−0.04
Δd_{34} (%)	−1.8	−0.9	−4.6	−4.6
Δh_4 (Å)	0.0	0.0	0.01	0.01

surface atom are comparatively larger for the C-terminated surfaces. For the Si as well as C surfaces, the top layer exhibits downward relaxation, whereas the second layer shows a relatively smaller upward displacement. This pattern repeats for the third and fourth layers. The vertical relaxations are found to be very small beyond the third layer.

B. Dimer formation on β-SiC(100)

As mentioned in the Introduction, the C-rich β-SiC(100) phase exhibits (2×1) reconstruction and is attributed to C-dimer formation on the surface plane.[34] The Si-rich phases, prepared by varying exposures to Si flux followed by annealing, show sequential (3×2), c(4×2), and (2×1), c(2×2), and (1×1) LEED patterns with a continuous Si depletion.[35] It has been proposed that the c(4×2) and (2×1) phases constitute one Si monolayer terminated surface.[35] By comparing with Si(100), which exhibits a transition from (2×1) to c(4×2) as the temperature is lowered below 200 K,[44] it has been suggested that both these phases consist of buckled dimers on their surfaces. These experimental observations lead to the conclusion that the monolayer C- or Si-terminated β-SiC(100) surfaces undergo dimerization on the surface layer, just as occurs on the (100) surfaces of group-IV solids.

Calculations for dimer formation on the β-SiC(100) surfaces were performed by using six-layer-thick infinite slabs. The unit cell consisted of 6 Si, 6 C, and 4 H atoms. The two neighboring Si (or C) atoms were allowed to relax laterally towards each other along the ⟨110⟩ direction with a simultaneous optimization of the interlayer distances for the top four layers. The dimer bond lengths and the vertical distances between layers were optimized to the nearest 0.01 Å. The calculated results are given in Table II. The side view of the Si-dimer terminated (100) surface is shown in Fig. 3. The calculations show that the relaxation patterns for the Si and the C surfaces of β-SiC(100) are quantitatively similar to those for the Si(100) and C(100) surfaces, respectively. The calculated Si-Si dimer distance of 2.16 Å is shorter than the bulk distance (2.36 Å) in silicon in part because of the smaller radius due to the larger Slater exponents used for the Si cations on the SiC surface. For the Si(100) surface, a variety of Si-dimer distances ranging from 2.25 to 2.57 Å have been derived,[1,12,13] but no comparison is available for the SiC surface. Surface dimer formation on β-SiC(100) also leads to changes in the interlayer spacings for a few surface layers, as given in Table II. The spacings alternate going into the bulk in the order decreasing, increasing, decreasing. The stability gain per Si dimer is calculated to be 1.03 eV, which is of the magnitude of 0.74 eV calculated by Takai *et al.*[37] The calculated densities of states before and after dimer formation on the Si terminated surfaces are shown in Fig. 4. When unrelaxed, the Si surface-state band is approximately 4.5 eV wide (from ~−6.5 to ~−11 eV in Fig. 4) and is merged with the top of the bulk band. The bottom 2 eV of the surface-

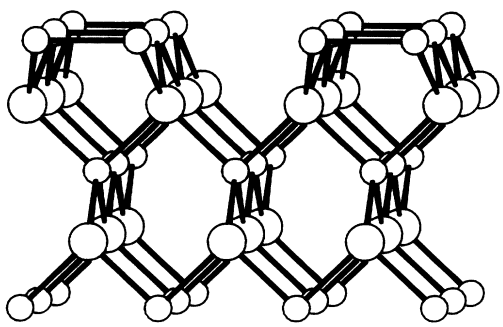

FIG. 3. (2×1) restructured β-SiC(100) Si-terminated surface.

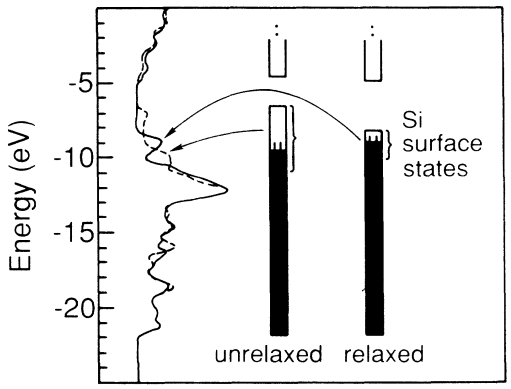

FIG. 4. The curves on the left show the calculated electronic density of states for unrestructured (dashed line) and (2×1) restructured (solid line) β-SiC(100) Si-terminated surfaces. These curves are from fitting Gaussian functions [full width at half maximum (FWHM) = 0.5 eV] to the calculated densities of states.

state band is composed of Si $3s,p$ hybrid orbitals perpendicular to the surface plane, while Si $3p$ orbitals parallel to the surface plane constitute the upper part of the surface-state band. As the neighboring Si atoms move laterally towards each other along the ⟨110⟩ direction to form symmetric dimer pairs, the total energy decreases due to the formation of an additional Si—Si bond in the surface layer by eliminating two dangling surface orbitals, one on each of the two Si atoms. The rehybridization of the dangling orbitals accompanying the dimer bond formation is shown qualitatively in Fig. 5. As may be seen from this figure, when the Si—Si σ bond (with a few percent π character) is formed, the corresponding antibonding orbital is pushed up high in energy and is emptied into the π-bonding orbital, resulting in a Si—Si bond order of 2. Each surface Si is now left with one dangling surface-state orbital which results in a surface-state band centered around −9.1 eV (Fig. 4).

The calculated C-C dimer distance on the relaxed C-terminated β-SiC(100) surface is 1.74 Å, which is longer

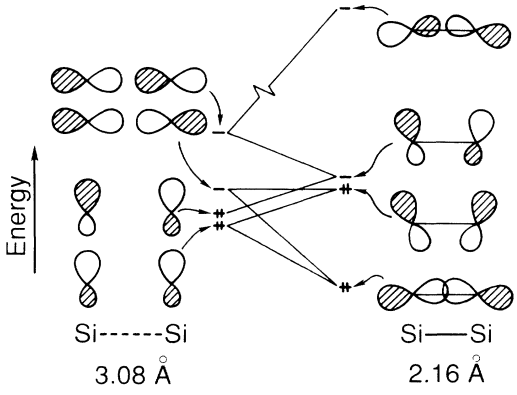

FIG. 5. Bonding interactions causing dimerization on Si-terminated β-SiC(100) surface as calculated from a small-cluster model.

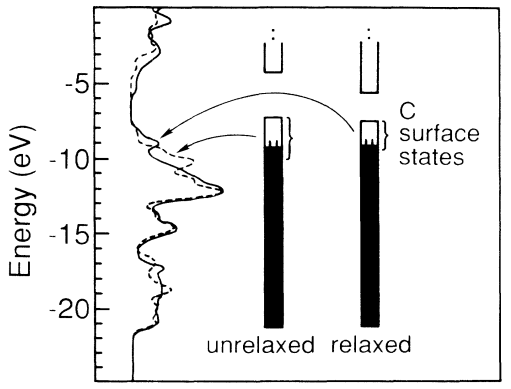

FIG. 6. As in Fig. 4 but for the C-terminated β-SiC(100) surfaces.

than the bulk C-C distance in diamond (1.54 Å). Again, there are no literature comparisons for SiC, but for diamond (100) calculations have yielded dimer distances ranging from 1.40 to 1.54 Å.[37,45–47] Our calculated dimerization energy of 1.22 eV is substantially less than 3.46 eV obtained by Takai *et al.*[37] using empirical potential functions. The calculated variations in the interlayer spacings for near surface layers associated with C-dimer formation are larger than those for the Si-dimer terminated surface, but show a similar trend. The densities of states for the unrelaxed C-covered surface and relaxed dimer terminated (100) surface are shown in Fig. 6. The former (shown by the dotted line) gives rise to approximately 3.0-eV-wide surface band (∼−7.2–∼−10.2 eV). The C $2sp_z$ hybrid orbitals normal to the surface plane, and the orthogonal C $2p_y$ orbitals lie, respectively, near the bottom 1.5 eV and the top 2 eV of the surface-state band. The interactions of the dangling surface orbitals on the (100) C surface resulting in C—C bond formation, and consequent elimination of two dangling surface orbitals, are qualitatively similar to that shown in Fig. 5. The resulting surface-state band is centered at about −9 eV.

IV. RELAXATIONS ON NONPOLAR SiC SURFACES

Three nonpolar surfaces with equal concentrations of Si and C atoms, β-SiC(110), α-SiC(10$\bar{1}$0), and α-SiC(11$\bar{2}$0) are considered. For the (110) and (11$\bar{2}$0) surfaces, each Si(C) is bonded to two C(Si) in the surface plane and to one C(Si) in the subsurface layer, resulting in chainlike structures. For the hexagonal (10$\bar{1}$0) surface, each surface Si(C) is bonded to one C(Si) in the surface plane and to two C(Si) in the layer underneath, giving this surface a SiC dimer-terminated appearance. Based on the atomic valence electronic structure arguments given before, since all these nonpolar surfaces have threefold-coordinated surface atoms these atoms should exhibit the driving force toward forming planar geometries with the atoms to which they are coordinated, resulting in inward displacements along the cleaved bond directions. We have carried out complete optimizations along the x, y, and z coordinates to the nearest 0.01 Å for the top two layer atoms to obtain minima in the potential-energy curves.

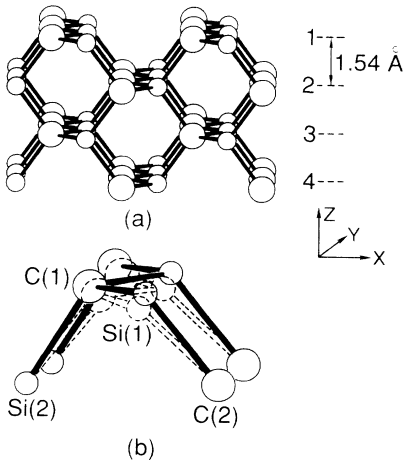

FIG. 7. (a) Four-layer slab of β-SiC with layer 1 representing a (110) surface. (b) Unrelaxed (solid line) and relaxed (dashed line) structures superimposed on each other.

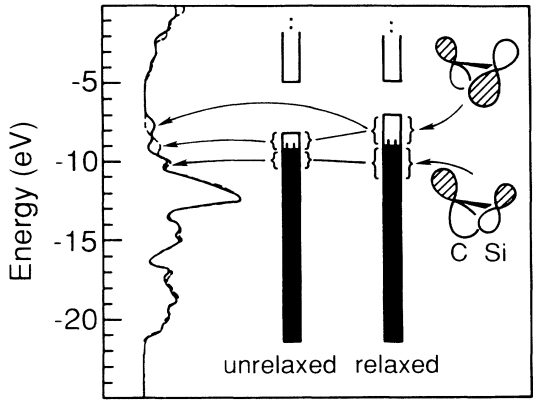

FIG. 8. As in Fig. 4 but for β-SiC(110). The C surface-state band is filled and the Si surface-state band is empty.

The results are presented in this section. The calculated surface relaxation energies are all less than 1 eV and are summarized and compared to the results of Lee and Joannopoulos[36] and Takai *et al.*[37] at the end of this section.

A. β-SiC(110)

The (110) surface of cubic SiC was modeled by a six-layer-thick slab, with one face saturated with H atoms. The unit cell had 6 Si, 6 C, and 2 H atoms. A perspective view of the surface is shown in Fig. 7(a). The calculated atomic displacements resulting from relaxations of the top two surface layers and relaxed geometry are given in Table III. The unrelaxed and relaxed positions of surface atoms are superimposed in Fig. 7(b). As expected, the surface Si and C atoms relax inward nearly along the direction of the cleaved bond. The inward displacement of Si atoms is calculated to be larger than that for C atoms, resulting in buckling of the surface layer. This causes the SiCSi and CSiC angles in the surface plane to increase from the tetrahedral angle (109.5°) for the ideal surface to 122° for the relaxed surface. As a result the zig-zag surface chain assumes a relatively straightened structure. The surface atoms are relatively closer to sp^2 hybridization for the relaxed surface structure. The Si—C bonds in the surface layer shrink to 1.76 Å, 0.13 Å less than the bulk value. About 97% of the stability obtained as a result of relaxation originates from the top surface-layer relaxation. The calculated densities of states for the ideal and relaxed surfaces are shown on the left-hand side of Fig. 8, and the electronic structures are on the right-hand side. For the unrelaxed surface, the occupied lower 1.2 eV of the surface-state band is constituted by orbitals with charge densities localized predominantly on surface C atoms. The C $2s,p$ hybrid orbitals have bonding π overlaps with the Si, $3s,p$ hybrid orbitals in the surface layer and are responsible for Si—C bond shrinkage in the surface plane. The upper empty portion of the surface-state band has orbitals which are mainly silicon in character. The Si $3s,p$ orbitals have antibonding overlaps with the C $2s,p$ orbitals on the neighboring surface atoms. These negative overlaps destabilize the Si surface-state band when the surface Si—C bond lengths decrease, as seen in Fig. 8.

TABLE III. Calculated structure parameters for surface relaxations on β-SiC(110) as shown in Fig. 7(b). Displacements are from the bulk positions. Cartesian axes are defined in Fig. 7. Labels 1 and 2 refer to the atoms in the surface and subsurface layers, respectively. Other semiempirical atom displacements calculated by Lee and Joannopoulos (Ref. 36) are in parentheses.

	Atomic displacements (Å)			
	C(1)	Si(1)	C(2)	Si(2)
ΔX	0.10(0.02)	−0.14(−0.14)	0.04(0.02)	−0.04(0.02)
ΔY	0.0(0.0)	0.0(0.0)	0.0(0.0)	0.0(0.0)
ΔZ	−0.12(−0.05)	−0.21(−0.17)	0.0(0.01)	−0.01(0.0)

Bond lengths (Å)	Bond angles (deg)
d(C(1)-Si(1))=1.76	θ(Si(1)-C(1)-Si) (surface plane)=122
d(C(1)-Si(2))=1.89	θ(Si(1)-C(1)-Si(2))=106
d(Si(1)-C(2))=1.84	θ(C(1)-Si(1)-C(2))=112

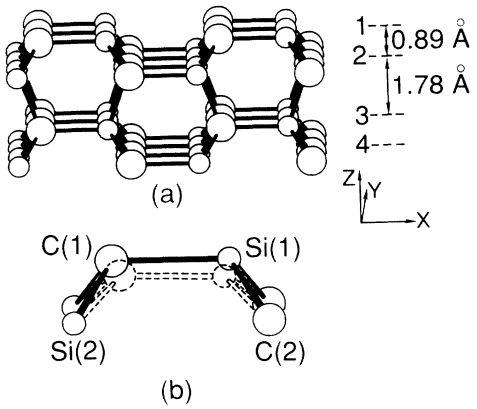

FIG. 9. (a) Four-layer slab of α-SiC with layer 1 representing the $(10\bar{1}0)$ surface. (b) As in Fig. 7(b) for the α-SiC$(10\bar{1}0)$ surface.

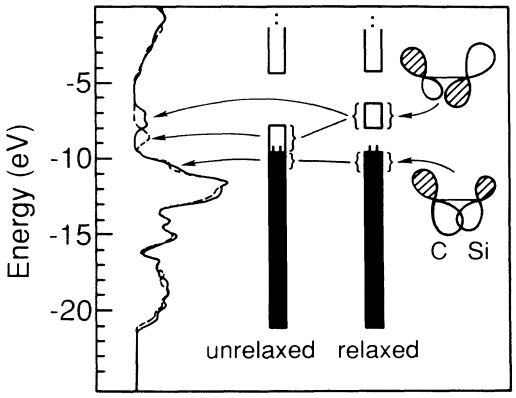

FIG. 10. As in Fig. 8 for the α-SiC$(10\bar{1}0)$ surface.

B. α-SiC$(10\bar{1}0)$

A six-layer-thick slab was employed for calculating relaxations on the top two surface layers on this surface. The unit cell consisted of 6 Si, 6 C, and 2 H atoms. A side view of the surface is shown in Fig. 9(a). The relaxation structures are in Table IV. The unrelaxed and relaxed atomic positions for the two surface layers are superimposed in Fig. 9(b). The surface Si and C atoms exhibit unequal downward displacements resulting in buckled and asymmetric SiC dimers on the surface layer. The Si-C dimer bond length is calculated to be 1.69 Å, which is 0.20 Å shorter than in the bulk. This shrinkage is due to the inphase π overlap between the *sp*-hybridized surface dangling orbitals on neighboring Si and C atoms which stabilizes the lower-lying filled C surface-state band. The empty surface-state band, which is predominantly Si in character, is destabilized due to the negative overlaps with the neighboring surface C atoms. The stabilization of the C surface-state band and the destabilization of the Si surface-state band (see Fig. 10) are relatively larger for this surface due to the favorable directions of the dangling surface states on the surface Si-C dimer atoms, resulting in stronger interactions. This explains the reason for the relatively larger relaxation energy for this surface compared to the other two nonpolar surfaces considered in this work. About 92% of the relaxation energy results from the top-layer relaxation. Figure 10 also shows on the left side the calculated densities of states for the ideal and relaxed $(10\bar{1}0)$ surface.

C. α-SiC$(11\bar{2}0)$

A three-layer-thick slab was used for calculating surface relaxations on the top two layers, with the third layer fixed at its bulk position. The unit cell had 6 Si, 6 C, and 4 H atoms. Figure 11(a) shows a side view of this surface. The calculated relaxation structures are given in Table V. In contrast to the results of surface-layer relaxations for the other two nonpolar surfaces where surface Si and C atoms were found to relax towards the bulk differently, resulting in buckling of the surface layer, we do not find any buckling on the α-SiC$(11\bar{2}0)$ surface plane. The SiCSi and CSiC angles in the relaxed surface layer increase to $\sim 118°$. There are two types of Si-C bond lengths on the relaxed surface plane: a short bond between C(1) and Si′(1) [see Fig. 11(b)] and comparatively long bonds between Si(1) and C(1) and Si′(1) and C′(1). It may be noted that this surface combines geometric features of the β-SiC(110) and α-SiC$(10\bar{1}0)$ surfaces. The *sp*-hybridized dangling surface-state orbitals on C(1) and Si′(1) are oriented in a way so as to form a strong π over-

TABLE IV. Calculated surface relaxations on α-SiC$(10\bar{1}0)$ as in Table III. See Fig. 9(b) for atom numbers and definitions of Cartesian axes. Other semiempirical atom displacements calculated by Lee and Joannopoulos (Ref. 36) are in parentheses.

	Atomic displacements (Å)			
	Si(1)	C(1)	Si(2)	C(2)
ΔX	−0.11(−0.08)	0.09(0.02)	−0.02(−0.02)	0.02(0.01)
ΔY	0.0(0.0)	0.0(0.0)	0.0(0.0)	0.0(0.0)
ΔZ	−0.22(−0.22)	−0.17(−0.14)	0.0(0.01)	0.05(0.01)

Bond lengths (Å)	Bond angles (deg)
d(C(1)-Si(1))=1.69	θ(C(1)-Si(1)-C(2))=113
d(C(1)-Si(2))=1.86	θ(Si(1)-C(1)-Si(2))=115
d(Si(1)-C(2))=1.84	

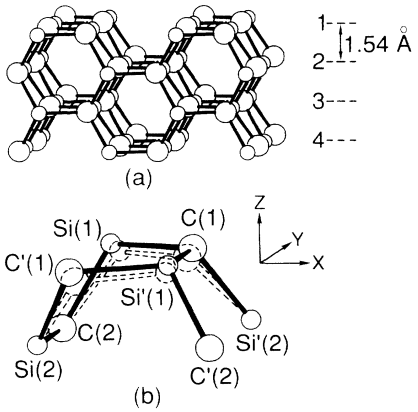

FIG. 11. (a) Four-layer slab of α-SiC with layer 1 representing the $(11\bar{2}0)$ surface. (b) As in Fig. 9(b) for the α-SiC$(11\bar{2}0)$ surface.

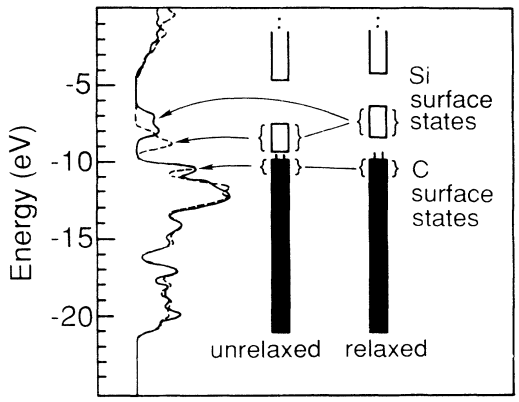

FIG. 12. As in Fig. 8 for the α-SiC$(11\bar{2}0)$ surface.

lap between them, resulting in a shorter bond [similar to α-SiC$(10\bar{1}0)$]. However, on [Si(1),C'(1)] and [Si'(1),C'(1)] pairs of atoms, the dangling orbitals are tilted in a manner that weakens π bond formation [similar to β-SiC(110)] resulting in comparatively longer bonds. The calculated relaxation energy per (Si,C) pair for this surface is also the average of the stabilities calculated for the β-SiC(110) and α-SiC$(10\bar{1}0)$ surfaces. About 96% of the relaxation stability originates from the surface layer. Figure 12 shows on the left the calculated densities of states for the ideal and relaxed surface, and on the right their electronic structures.

D. Relaxation energies for the nonpolar surfaces

Table VI compares our calculated relaxation energies for the nonpolar (110), $(10\bar{1}0)$, and $(11\bar{2}0)$ surfaces with the semiempirical calculations of Lee and Joannopoulos[36] and the empirical extrapolations of Takai *et al.*[37] Our energies are roughly twice those obtained by Lee and Joannopoulos and are all less than 1 eV. Takai *et al.* studied only (110) surface relaxations and the 0.76 eV/dimer energy is relatively close to our calculated energy of 0.64 eV/dimer. The most that can be concluded from these comparisons is that the relaxation energies for these surfaces are probably less than 1 eV.

V. CONCLUDING REMARKS

We have calculated atomic relaxations on the polar (111) and (100) β-SiC surfaces, and the nonpolar β-SiC(110), α-SiC$(10\bar{1}0)$, and α-SiC$(11\bar{2}0)$ surfaces using a tight-binding approach. Relaxations on the α-SiC(0001) surface should be comparable to those on the β-SiC(111) because of structural similarity between the two surfaces. The Si- and C-terminated (111) surfaces exhibit multilayer relaxations resulting in contraction of the spacing in the double layers and expansion of the spacing between the double layers. The C surface shows relatively larger displacements for the top few layers. Takai *et al.*,[37] using empirical potential-energy functions in a Monte Carlo scheme, reached the same conclusion regarding the relative relaxations of the Si- and C-terminated β-SiC(111)

TABLE V. Calculated surface relaxations on α-Si$(1\bar{1}20)$ as in Table III. See Fig. 11(b) for atom numbers and definition of Cartesian axes. Other semiempirical displacements calculated by Lee and Joannopoulos (Ref. 36) are in parentheses.

	Atomic displacements (Å)							
	Si(1)	C(1)	Si'(1)	C'(1)	Si(2)	C(2)	Si'(2)	C'(2)
ΔX	0.09	−0.09	−0.09	0.09	−0.02	−0.02	0.02	0.02
	(0.06)	(−0.04)	(−0.06)	(0.04)	(−0.11)	(−0.02)	(0.02)	(0.01)
ΔY	0.11	−0.11	0.11	−0.11	0.02	−0.02	0.02	−0.02
	(0.04)	(−0.05)	(0.04)	(−0.05)	(0.01)	(0.01)	(0.01)	−(0.01)
ΔZ	−0.07	−0.17	−0.17	−0.17	0.0	0.0	0.0	0.0
	(−0.12)	(−0.07)	(−0.12)	(−0.07)	(0.01)	(0.01)	(0.01)	(0.01)

Bond lengths (Å)

d(Si(1)-C(1))=1.81=d(Si'(1)-C'(1))
D(C(1)-Si'(1))=1.68
d(Si(2)-C(2))=1.85
d(Si(1)-C(2))=d(Si(1)-C'(2))=1.85
d(C(1)-Si'(2))=d(C(1)-Si(2))=1.85

Bond angles (deg)

θ(Si(1)-C(1)-Si'(1))=118=θ(C(1)-Si'(1)-C'(1))

TABLE VI. Calculated stability gains (eV/SiC pair) resulting from surface relaxations for the nonpolar β-SiC(110), α-SiC($10\bar{1}0$), and α-SiC($11\bar{2}0$) surfaces.

Surface	Present work	Lee and Joannopoulos[a]	Takai *et al.*[b]
(110)	0.64	0.42	0.76
($10\bar{1}0$)	0.94	0.48	
($11\bar{2}0$)	0.77	0.36	

[a]Reference 36.
[b]Reference 37.

surface, though they did not give details of their calculated relaxations. The Si and C surfaces of β-SiC(100) display dimer formation on the surface layer along with multilayer inward displacements, a behavior that closely resembles that of Si(100) and C(100) surfaces, respectively.

Among the nonpolar surfaces, the β-SiC(110) surface relaxations result in buckling of the surface layer due to the relatively larger inward displacement of Si atoms than C atoms. This result agrees with the calculations of Lee and Joannopoulos.[36] This type of buckling for a binary material has been known for GaAs(110)[48,49] which has the same structure as β-SiC(110).

The ($10\bar{1}0$) surface of hexagonal SiC exhibits asymmetric and buckled SiC dimers on the surface. The short dimer distance is found to be due to π overlap between *sp*-hybridized dangling surface orbitals on the Si and C atoms. The α-SiC($11\bar{2}0$) surface shows relaxation trends which are the average of those exhibited by β-SiC(110) and α-SiC($10\bar{1}0$). This has been explained on the basis of its surface structure and consequent orientations of the dangling surface state orbitals on near-neighbor atoms, which involve features common to the other two nonpolar surfaces studied here.

ACKNOWLEDGMENTS

This work has been supported by a grant to Case Western Reserve University from the U.S. Defense Advanced Research Projects Agency administered by the Office of Naval Research and by the U.S. National Science Foundation through Grant No. DMP 89-03527.

*Author to whom correspondence should be addressed.

[1]W. S. Yang, F. Jona, and P. M. Marcus, Phys. Rev. B **28**, 2049 (1983), and references therein.
[2]B. W. Holland, C. B. Duke, and A. Paton, Surf. Sci. **140**, L269 (1984).
[3]A. Goldman, P. Koke, W. Mönch, G. Wolfgarten, and J. Pollmann, Surf. Sci. **169**, 438 (1986).
[4]P. Martensson, A. Cricenti, and G. V. Hansson, Phys. Rev. B **33**, 8855 (1986).
[5]R. J. Hamers, R. M. Tromp, and J. E. Demuth, Phys. Rev. B **34**, 5343 (1986).
[6]H.-S. Jin, T. Ito, and W. M. Gibson, J. Vac. Sci. Technol. A **4**, 1385 (1986).
[7]D. H. Rich, A. Samsavar, T. Miller, H. F. Lin, T.-C. Chiang, J. E. Sundgren, and J. E. Green, Phys. Rev. Lett. **58**, 579 (1987).
[8]D. H. Rich, T. Miller, and T.-C. Chiang, Phys. Rev. B **37**, 3124 (1988).
[9]J. G. Nelson, W. J. Gignac, R. S. Williams, S. W. Robey, J. G. Tobin, and D. A. Shirley, Phys. Rev. B **27**, 3924 (1983).
[10]T. C. Hsieh, T. Miller, and T.-C. Chiang, Phys. Rev. B **30**, 7005 (1984).
[11]D. J. Chadi, Phys. Rev. Lett. **43**, 43 (1979); Phys. Rev. B **19**, 2074 (1979).
[12]W. S. Verwoerd, Surf. Sci. **99**, 581 (1980); **103**, 1104 (1981).
[13]M. T. Yin and M. L. Cohen, Phys. Rev. B **24**, 2303 (1981).
[14]A. Mazur and J. Pollmann, Phys. Rev. B **26**, 7086 (1982).
[15]F. F. Abraham and I. P. Batra, Surf. Sci. **163**, L752 (1985).
[16]F. Bechstedt and D. Reichardt, Surf. Sci. **202**, 83 (1988).
[17]P. Krüger, A. Mazur, J. Pollmann, and G. Wolfgarten, Phys. Rev. Lett. **57**, 1468 (1986).
[18]J. Ihm, M. L. Cohen, and D. J. Chadi, Phys. Rev. B **21**, 4592 (1980).
[19]J. Ihm, D. H. Lee, J. D. Joannopoulos, and J. J. Xiong, Phys. Rev. Lett. **51**, 1872 (1983).
[20]E. Artacho and F. Yndurain, Phys. Rev. Lett. **62**, 2491 (1989).
[21]B. I. Craig and P. V. Smith, Surf. Sci. **218**, 569 (1989).
[22]I. P. Batra, Phys. Rev. B **41**, 5048 (1990).
[23]D. Haneman, Adv. Phys. **31**, 165 (1982), and references therein; Rep. Prog. Phys. **50**, 1045 (1987), and reference therein.
[24]F. J. Himpsel, D. E. Eastman, P. Heimann, and J. F. van der Veen, Phys. Rev. B **24**, 7270 (1981).
[25]F. Houzay, G. Guichar, R. Pinchaux, G. Jezequel, F. Solal, A. Barsky, P. Steiner, and Y. Petroff, Surf. Sci. **132**, 40 (1983).
[26]J. M. Nicholls, G. V. Hansson, R. I. G. Uhrberg, and S. A. Flodstrom, Phys. Rev. B **27**, 2594 (1983).
[27]W. S. Yang and F. Jona, Phys. Rev. B **29**, 899 (1984).
[28]G. D. Kubiak and K. W. Kolasinski, Phys. Rev. B **39**, 1381 (1989).
[29]K. C. Pandey, Phys. Rev. Lett. **47**, 1913 (1981); Phys. Rev. B **25**, 4338 (1982).
[30]D. Haneman, Phys. Rev. **121**, 1093 (1961).
[31]R. Seiwatz, Surf. Sci. **2**, 473 (1964).
[32]D. J. Chadi, Phys.Rev. B **26**, 4762 (1982).
[33]D. Vanderbilt and S. G. Louie, Phys. Rev. B **30**, 6118 (1984).
[34]M. Dayan, J. Vac. Sci. Technol. A **3**, 361 (1985); **4**, 38 (1986).
[35]R. Kaplan, Surf. Sci. **215**, 111 (1989).
[36]D. H. Lee and J. D. Joannopoulos, J. Vac. Sci. Technol. **21**, 351 (1982).
[37]T. Takai, T. Halicioglu, and W. A. Tiller, Surf. Sci. **164**, 341 (1985).
[38](a) A. B. Anderson, J. Chem. Phys. **62**, 1187 (1975); (b) A. B. Anderson, R. W. Grimes, and S. Y. Hong, J. Phys. Chem. **91**, 4245 (1987).
[39]E. Clementi and D. L. Raimondi, J. Chem. Phys. **38**, 2686 (1963).
[40]W. Lotz, J. Opt. Soc. Am. **60**, 206 (1970).
[41]K. Nath and A. B. Anderson, Solid State Commun. **66**, 277

(1988); Phys. Rev. B **41**, 5652 (1990).
[42]K. Nath and A. B. Anderson, Phys. Rev. B **40**, 7916 (1989).
[43]S. P. Mehandru and A. B. Anderson (unpublished).
[44]T. Tabata, T. Aruga, and Y. Murata, Surf. Sci. **179**, L63 (1987).
[45]S. P. Mehandru and A. B. Anderson (unpublished).
[46]W. S. Verwoerd, Surf. Sci. **99**, 581 (1980); **103**, 404 (1981).
[47]F. Bechstedt and D. Reichardt, Surf. Sci. **202**, 83 (1988).
[48]P. Mark, G. Cisneros, M. Bonn, A. Kahn, C. B. Duke, A. Paton, and A. R. Lubinsky, J. Vac. Sci. Technol. **14**, 910 (1977).
[49]C. B. Duke, R. J. Mayer, A. Paton, P. Mark, A. Kahn, E. So, and L. J.Yeh, J. Vac. Sci. Technol. **16**, 1252 (1979), and reference therein.